Research Article

Journal of Environmental Nanotechnology

Modelling of a 70 MHz SAW Filter for Potential Applications in Mobile Communication Systems

T. Venkatesan[1], R. Banu Priya[2], P. Gowdhaman[1], Haresh M. Pandya[1]*

[1]*Department of Physics, Chikkanna Government Arts College, Tiruppur, TN, India*
[2]*Department of Physics, Gobi Arts and Science College, Gobichettipalayam, TN, India*
Received: 08.01.2018 Accepted: 22.02.2018
*haresh.pandya@rediffmail.com

ABSTRACT

In the present paper, a 70 MHz $LiNbO_3$ SAW filter device is designed, modelled and simulated. The frequency sampling methods and the windowing methods are adopted, and using a user-defined MATLAB® simulation tool was employed for developing the algorithms. A computationally simulated frequency response of 70 MHz SAW filters has compared with the experimental device result. These device responses utilized and implemented during the design and development stage of these devices for their potential applications in mobile communication systems (GSM/CDMA/WCDMA) for filtering the higher order as well as intermediate frequencies.

Keywords: SAW Filter; Communication; MATLAB; Window functions.

1. INTRODUCTION

Surface Acoustic Wave (SAW) devices such as SAW delay lines, SAW filters, SAW resonators etc., are performed a vital role in different fields. Among these devices, the SAW filter is one of the basic needs of digital signal processing (DSP) applications: digital signal filtering, image processing techniques (Parker, 2014), noise reduction, frequency analysis, multimedia compression radio frequency identification tags (RFID), fibre optics, micro radio and satellite transmission devices, etc. They are the main components to obtain the high performance in the communication systems: cellular radio, mobile, cordless and portable telephone, wireless systems and touchscreen devices (Luo *et al.* 2016). For mobile phones, it contains two or more distinct SAW filters are used for filtering both radio frequency (RF) and intermediate frequency (IF) (Campbell, 1989a). These filters are attempted in telecommunication systems such as mobile telephone transceivers, Environmental sensors, cable TV repeaters and converters (Hikita *et al.* 2006). Thus, SAW filter devices have become indispensable and gaining importance in the modern electronics industry as the world goes wireless (Venkatesan and Haresh, 2013).

Generally, filters are classified into four categories. There are (i) low pass filter, (ii) high pass filter, (iii) bandpass filter and (iv) band-stop filter. Particularly, a SAW filter is a bandpass filter category, and it passes some desired signal to reduce or enhance the features of the given signal and more than others. A typical SAW bandpass filter device range values are given in table 1. The choice of the piezoelectric substrate is basic: to the realization of filter specifications, including tradeoffs between insertion loss, fractional bandwidth, temperature stability, shape factor (= 1 is ideal) etc.,(Campbell, 1989a). These filter specifications used to pass the frequency signals according to the specified requirements: bandpass filter, stop-band rejection, low insertion loss and high sidelobe suppression. The response of a bandpass filter consists of a passband, the transition bands in which the signal attenuation falls to the required rejection level, and the stopband (SB). The width of the passband is typically defined as either the relative bandwidth to the minimum insertion loss or the absolute 3dB bandwidth.

SAW bandpass filters are aided as front-end receivers in the VHF and UHF regions (Hikita *et al.* 2006). Moreover, it can be made to operate very efficiently at higher harmonic frequencies. Thus, the performance of the SAW filter is important in the device design parameters.

This paper discusses the concepts and ideas of digital signal processing (DSP) techniques. Then, they are inferred and applied to the design of the SAW device and traces the device simulation process (Laker *et al.* 1978). These processes are adopted by the impulse response model, including windowing and frequency sampling methods (Hartmann, 1973). However, the majority of known optimization algorithms are effective for apodized IDTs with a large number of electrode pairs and a bandwidth of 1% or less (Bausk and Yakovkin, 1996). This limitation is caused by accepted approaches to optimization of the device structure for an approximation of a desired IDT impulse

response(Hartmann, 1973; Laker *et al.* 1978; Yatsuda and Yamanouchi, 2000). When the number of electrode pairs is large enough (>100), this method guarantees a good coincidence of IDT frequency response with the desired shape, atleast in frequency regions close to passband (Bausk and Yakovkin, 1996).

Table 1. Types of a SAW bandpass filter and their parameter values

Parameter	Bidirectional Filter	Low-loss Filter	Low-loss Wideband filter
Fractional Bandwidth % (BW)	0.1 to 67%	0.1 to 8%	1 to 67 %
Insertion loss	-15 to -35 dB	-2 to -15 dB	-5 to -15dB
Ultimate Rejection	40 to 70 dB	25 to 60 dB	40 to 60 dB
Shape Factor	1.15 to 4.0	1.5 to 4.0	1.15 to 4.0

In this context, the computer simulation method provides fast response, reliable and inexpensive. This method utilized to enhance the SAW filter device performance. It can also make repeated modifications of the design parameters with ease to obtain the desired frequency response. In the present research study, the input parameters optimized for the device design to give a complete response of 70 MHz SAW filter. The SAW filter was codified using the MATLAB® algorithm by realizing the impulse response model equations. Then, the theoretically modelled responses compared with available experimental results online.

2. SAW FILTER DESIGN, MODELLING AND SIMULATION PROCESS

2.1 Basic SAW Theory for Simulation by Impulse Response Model

An impulse response is created by impulse signals fed to the input transducer, which again appears as an impulse at the output transducer (Venkatesan and Haresh, 2013; Fall *et al.* 2015). Thus, the impulse signal strength depends mainly on the interdigital transducer (IDT) electrode geometry and its periodicity(*p*). However, it is including the amount of SAW energy radiated and is proportional to the finger overlap or aperture (*w*) of the IDT (Morgan, 1973). The impulse response is basically a function of the time period and represented in the time domain. The time-domain response obtained corresponding to each IDT finger/electrode location. Fig. 1, shows the relation between the time domain response obtained at different finger/electrode locations (Peroulis *et al.* 2016). An alternatively, the device response is looking in terms of its frequency response in the frequency domain, which is obtained mathematically from the time-domain impulse response by performing a Fourier transform (Harris, 1978), (Priya *et al.* 2016) since the low signals can be resolved in the frequency domain because it would never be visible in the time-domain by using the logarithmic amplitude scale. The relation between the time domain and the frequency domain function shown in fig. 2.

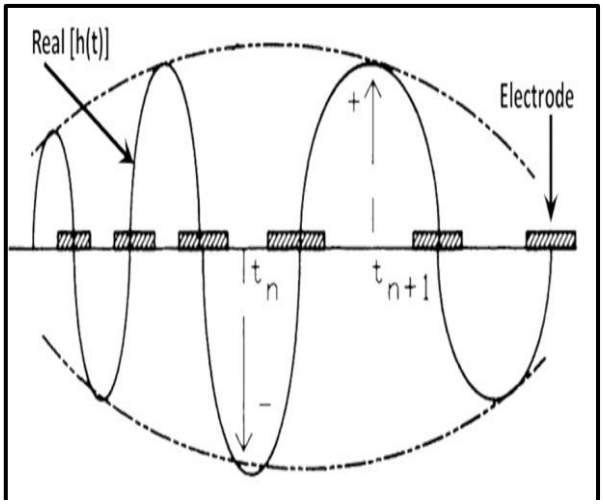

Fig. 1: The relation between time samplings and metal electrode

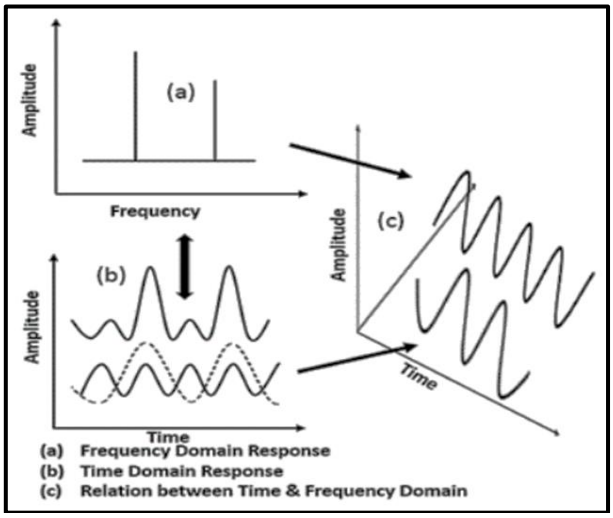

Fig. 2: The relation between time domain and frequency domain function

The time domain is consisting of N cycles of device operating frequency f_0. It includes the number of finger pairs (N) in the IDT, periodicity or the uniform electrode spacing of the IDT structure (λ_0), the surface wave velocity (v) and the length of either input/output IDT ($N\lambda_0$). Therefore, the time domain T is

$$T = Nt = \frac{N}{f_0} = \frac{N\lambda_0}{v}$$

If the impulse response of the device is represented as *h(t)* in the time domain and *H(f)* in the frequency domain, then since both of them are equivalent representations, mathematically, they formed with a Fourier pair. The impulse response *h(t)* can be mathematically represented as

$$h(t) = \frac{1}{2\pi}\int_{-\infty}^{+\infty} H(f)e^{j2\pi ft}df$$

The frequency response *H(f)* is mathematically represented as

$$H(f) = \int_{-\infty}^{+\infty} h(t)e^{-j2\pi ft}dt$$

Where the evaluation of the impulse response *h(t)*and the frequency response *H(f)* is over the range of $-\infty \le f \le +\infty$ and $-\infty \le t \le +\infty$ respectively.

To obtain the desired frequency response, the inverse Fourier transform of the steady-state frequency response taken, which provides the impulse response in the time domain. A sampling of this result yields the sampling times t_n. The electrodes can then be conveniently positioned (x_n) at the zero crossings of the impulse response at time t_n given by $x_n = vt_n$. It generates the complete spatial and geometric pattern of the IDT device with exact details of electrodeposition and periodicity (fig. 1).

2.1.1 Sampling Theorem

The IDT finger location can be constructed efficiently by means of the sampling theorem, which is also called as Nyquist Sampling Theorem (Atzeni and Masotti, 1973; Panasik and Hunsinger, 1976). It states that *"the frequency of signal sampling f_s must be at least twice faster than the highest signal frequency component (denoted as f_h)to accurately reconstruct the original continuous-time signal, i.e. $f_s > 2f_h$"* (Nyquist 1928).

2.1.2 Fast Fourier Transforms (FFT)

Fourier Transforms is a mathematical as well as computational algorithm. It is developed to improve computational efficiency and is the most popular method used in spectral analysis and digital signal processing (DSP) techniques (Harris, 1978). Thus, the SAW filter frequency response can be established by using the discrete Fourier transforms (DFT), and fast Fourier transforms (FFT). DFT is compared with FFT, and it has a high computation time. Any computation using DFT, it requires $2N^2$ calculations to be done. For example, a 2000 point DFT requires 4 million calculations. Therefore, DFT is a slow process algorithm (Cooley and Tukey, 1965). This problematic DFT can be avoided by the utilization of the Fast Fourier Transform (FFT). FFT perform as remedies the DFT speed problem by skipping over portions of the summations that they produce redundant information (Cooley and Tukey, 1965). In FFT, it's required only that the proper implementation of the mathematical algorithm. It includes the number of sample points N be a power of 2 (2^N). Thus, the computing time also found to be proportional to $N\log_2(N)$.

2.2 Design of SAW filter

In the design of the SAW filter, apodization or finger overlap is the most flexible and suitable method for the realization of specified IDT frequency response. The input apodized IDT can provide a very low-frequency response shape factor, but its experimental stopband rejection doesn't exceed 30-35 dB (Bausk and Yakovkin, 1996).In case a uniform electrode structure output IDT and unweighted time response has a poor frequency selectivity (Bausk and Yakovkin, 1996). Because of bad frequency response, it adds a significant value to stopband rejection of input transducer only in frequency regions far from its passband (Bausk and Yakovkin, 1996). Therefore, the usage of apodized IDT improve the selectivity of unapodized transducers.

In this case, the SAW filter includes only two selective elements: input and output apodized IDTs used with respect to the window functions. The IDT structures served to suppress the spurious sidelobe levels in the frequency response. These responses produced by the electrodes and/or the area are varied. The principle of varying electrode length is used in bandpass filters, whereas that for changing areas is used in chirp filters (Fig. 4). With the limitations of fabrication technology, any desired frequency response can be realized in the SAW filter (Venkatesan and

Pandya, 2013). Thus, the SAW device can be enabled to process an applied electrical signal by rejecting the unwanted frequency components. Therefore, the electrode lengths varied by using window functions in the fabrication process.

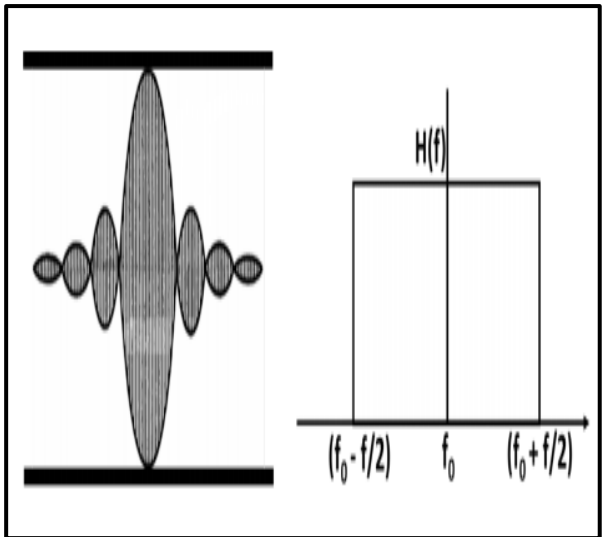

Fig. 3: A Sinc Window of IDT and Frequency Response

SAW filter designs with different types of standard window functions are used in the IDT geometry to enhance the desired frequency response. The window functions are Bartlett window, Blackman window, Hamming Window, Hanning Window, Kaiser window, Rectangular window, Taylor window, Triangular window etc., (Harris, 1978; Parker, 2014; AVCİ, 2016; Kaur and Sangeet, 2016), can be incorporated in the designing process of the IDT structure as shown in fig.3. Moreover, each window functions have their own properties with including the mathematical equations. Some mathematical relation of the window function is given below.

Hamming Window Equation (Harris, 1978):

$$w(n) = 0.54 - 0.46\cos\left(2\pi\frac{n}{N}\right), 0 \le n \le N$$

Hanning Window Function (Harris, 1978):

$$w(n) = 0.5\left[1 - \cos\left(2\pi\frac{n}{N}\right)\right], 0 \le n \le N$$

Where N is the number of sampling of the input IDT sequence and the number of frequency points in the FFT output, N can be any positive integer, but the order of 2^N is usually chosen, i.e., 128, 256, 512, 1024, etc., and n is the time domain index of the input sampling, and its values can be taken as0, 1, 2,3,…, N-1.

Sinc window function is

$$\text{sinc} = \left(\frac{\sin X}{X}\right), \text{ where } X = N_P\pi\left[\frac{f - f_0}{f_0}\right]$$

N_P is the number of IDT finger pairs and f is the instantaneous frequency at any instant of time t.

Therefore, the impulse response model based SAW filter frequency response has been evaluated by time-domain response equation(Hartmann *et al.* 1973) and is given by,

$$h(t) \alpha 4\sqrt{K^2 C_s}\, f_0^{3/2}(t)\sin(2\pi f_0 t)$$

Where $K^2$is the coupling coefficient of the piezoelectric material, C_S is the IDT electrode pair static capacitance per unit length (pf/cm-pair) and $f_0$is the center frequency of operation. Now, taking the Fast Fourier Transform (FFT) of equation (5) we get,

$$H(f) = 20\log\left|\left[4K^2 C_s W f_0 N_P^2\left(\frac{\sin X}{X}\right)^2 e^{-i\left(\frac{N_P+D}{f_0}\right)}\right]\right|$$

Where W is the window function of the IDTs, D is the delay length in wavelengths between the IDTs. For example, a schematic diagram of SAW filter IDT with time domain and frequency domain responses of input IDT (as unapodized) and output IDT (as apodized) are shown in fig. 4.

The above equations are effectively used to obtain the frequency response of a SAW filter device with the help of a MATLAB® simulation tool. The basic parameters need to design the SAW filter as follows,

(i) Structure of electrode geometry types, split or double electrode,
(ii) Number of finger pairs in the input IDT '*M*',
(iii) Number of finger pairs in the output IDT '*N*',
(iv) Finger gaps between adjacent electrodes '*D*',
(v) IDT center to center distance '*L*',
(vi) Type of apodization or window function *'W(n)'* (Ex. Hamming, Hanning and Sinc).

The frequency response of the experimentally fabricated SAW device has tested using a vector network analyzer (VNA) to confirming the device design parameters.

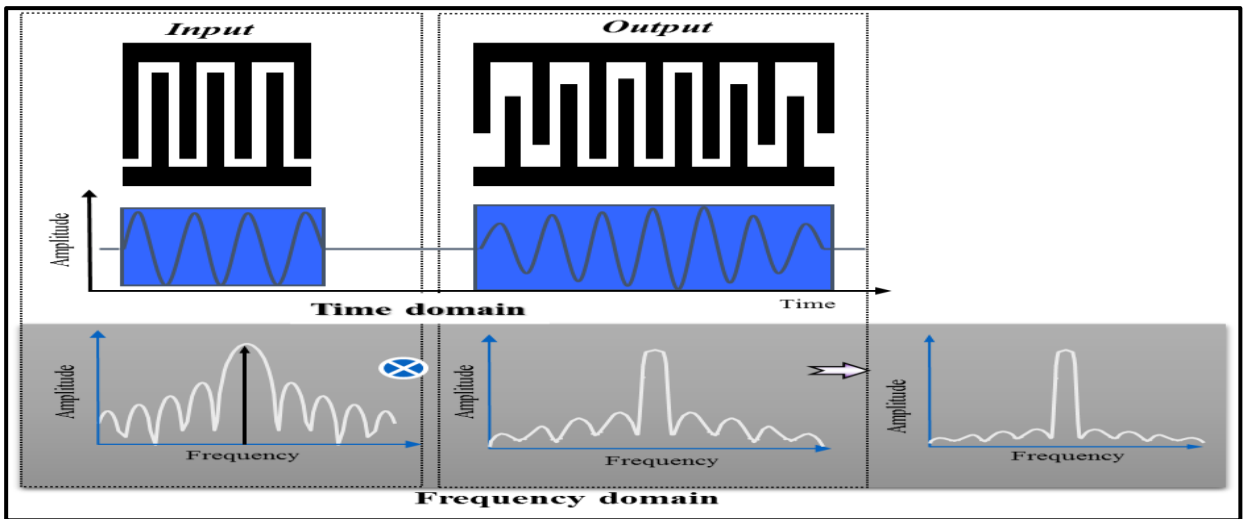

Fig. 4: Time and Frequency Domain Response of SAW filter IDT

The above equations are effectively used to obtain the frequency response of a SAW filter device with the help of a MATLAB® simulation tool. The basic parameters need to design the SAW filter as follows,

(vii) Structure of electrode geometry types, split or double electrode,
(viii) Number of finger pairs in the input IDT '*M*',
(ix) Number of finger pairs in the output IDT '*N*',
(x) Finger gaps between adjacent electrodes '*D'*,
(xi) IDT center to center distance '*L*',
(xii) Type of apodization or window function *'W(n)'* (Ex. Hamming, Hanning and Sinc).

The frequency response of the experimentally fabricated SAW device has tested using a vector network analyzer (VNA) to confirming the device design parameters.

2.3 Modelling of SAW filter

The following steps are involved in the modelling of the SAW filter,

(i) To define the SAW filter specifications (like bandpass).
(ii) To specify the window functions according to the filter specifications.
(iii) To compute the filter order required for a given set of specifications.
(iv) To compute the SAW filter according to the obtained window function.
(v) If the resulting SAW filter has too wide or too narrow transition region, it is necessary to change the SAW filter order by increasing or decreasing it according to the needs, and after that, the step (iii) and (iv) are iterated as many times as needed for the requirement.

2.4 Modelling Strategy of the present study

A few numbers of steps adapted for modelling of SAW filter devices are highlighted as follows:

1. The realization of a good selectivity in SAW filters on good piezoelectric material as lithium niobate ($LiNbO_3$) is preferable (Bausk and Yakovkin, 1996). The penetration of the SAW into the piezoelectric is about one acoustic wavelength λ. It has a good surface wave velocity to travel the waves long time period with negligible passband ripple (Peach and Dix, 1978). Moreover, compared to other substrates, $LiNbO_3$ substrate has affordable for utilization of a SAW filter construction with input and output apodized IDTs (Bausk and Yakovkin, 1996). Hence, a high-quality YZ-$LiNbO_3$ substrate was selected (Campbell, 1989b).

2. The structure of IDT has designed in the form of Hamming window, Hanning Window and Sinc Window. The IDT is made up of Aluminium (Al) material because it serves as good inert and adhesive metal (Budreau 1971).

3. In the analysis of the Fourier transform of these different window functions, for the fixed-length, the Hamming, Hanning and Sinc window have significantly lower sidelobe amplitude, but the main lobe width is wider compare to the Rectangular window.

4. Before implementation of the Impulse Response model chosen by the device designer, the

following input parameters have to be chosen to analyze the SAW device. The basic input parameters in the present study are tabulated in table 2, and the MATLAB® algorithm was developed for 70 MHz SAW Filter.

Table 2. Input Parameters for the Modelling Study

S.No	Name of the parameter	Symbol	Value
1	Coupling coefficient	K^2	0.049 (YZ $LiNbO_3$)
2	Surface Velocity	v_s	3488 m/s
3	The capacitance of Finger pair/unit length	C_s	4.5 x 10^{-10} F/m
4	Central Frequency	F_0	70MHz
5	Number of IDT Finger Pair	N_p	100
6	Width of Finger or Gap in IDT	d	12.4571x 10^{-6}m
7	Load Resistance	R_L	50Ω

3. RESULTS AND DISCUSSION

MATLAB® algorithms are codified using the above-given equations through an impulse response model for the optimization of SAW filter design. Then, the modelled algorithms are generated the output response of the 70 MHz SAW filter. In the present modelling study, three types of SAW filter device simulations were carried out, including double electrode geometry having 100 electrode pairs in both input and output IDTs. The SAW filter output responses are graphically obtained, and the magnitude values are found for the insertion loss, 3dB bandwidth, fractional bandwidth and shape factor.

In the first study, the SAW filter was modelled for the apodized IDTs, i.e. the input IDT is a hamming window function, and the output IDT is the Sinc window function. The modelled output response of the SAW filter is used to filtering the wideband device, including ultimate rejection as shown in fig. 5.

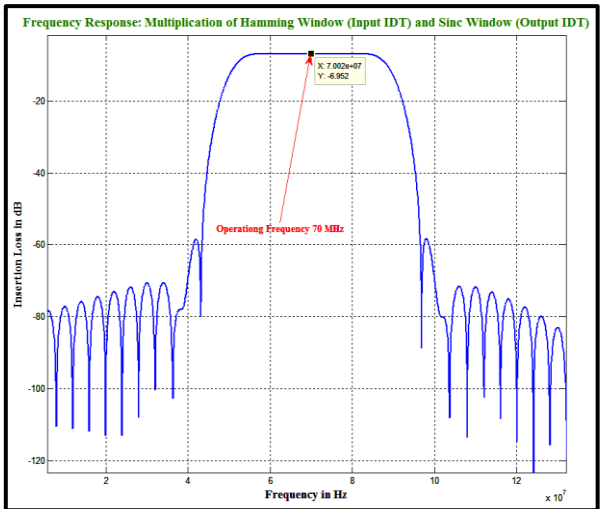

Fig. 5: Modelled Output Frequency Response for 70 MHz SAW Filter

In the second study, the SAW filter was modelled for the same apodized IDTs, but the input IDT is chosen as Hanning window function only. The modelled output response of the SAW filter is shown in fig. 6. The Hanning window function result gives much less than the previous device response, and they reduce the filtering capacity of the desired frequencies in the SAW filter.

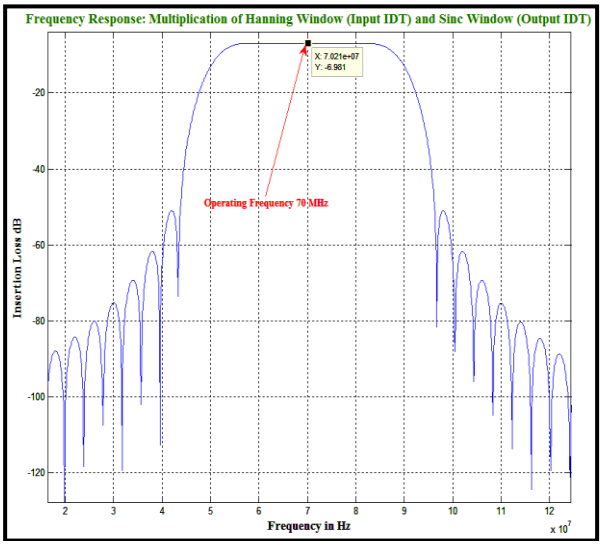

Fig. 6: Modelled Output Frequency Response for 70 MHz SAW Filter

In the third study, the SAW filter was modelled for both IDTs are apodized as Sinc window function. The modelled output response of the SAW filter is shown in fig.7. The Sinc window function result is given a greater responsibility which is compared to other modelled device responses. It produces a larger bandwidth and lower insertion loss in the desired frequency.

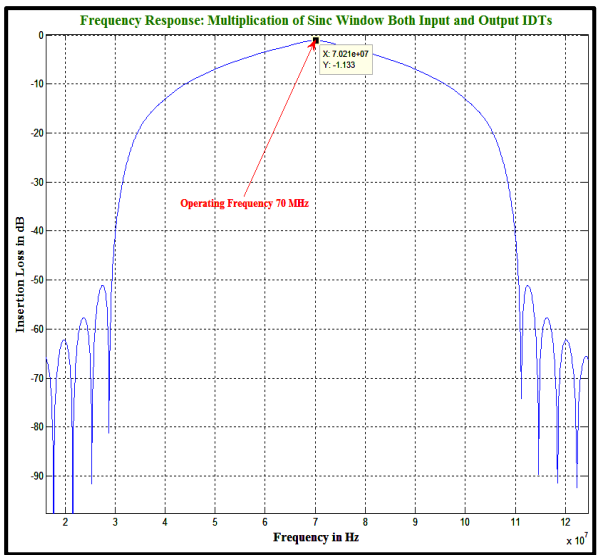

Fig. 7: Modelled Output Frequency Response for 70 MHz SAW Filter

3.1 Experimental Results and Comparison:

The obtained modelled results are compared with experimental results available from Advanced Microwave Technologies (AMT), Korea (web resource ([CSL STYLE ERROR: reference with no printed form.])) for a 70 MHz YZ-$LiNbO_3$ SAW filter device which has been developed for mobile communication systems is represented in fig. 8.

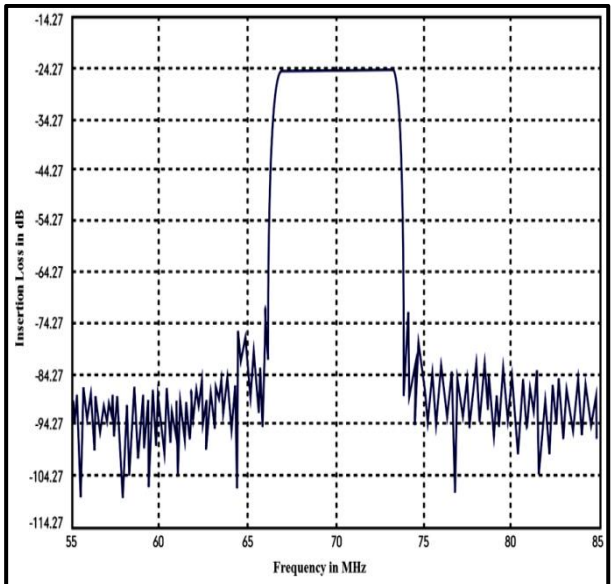

Fig. 8: Experimentally calculated Frequency Response for 70 MHz SAW Filter ([CSL STYLE ERROR: reference with no printed form.])

Table 3 summarizes the performance of the theoretically presented and the experimentally tested insertion loss and 3dB bandwidth values of the 70 MHz YZ-$LiNbO_3$ SAW filter. It shows that this work realizes a much wider bandwidth and low insertion loss of the SAW filter.

Table 3. Comparison of Modelled and Experimental Output Results

	Insertion Loss (dB)	3dB Bandwidth (MHz)	Fractional 3dB Bandwidth	Shape Factor
Study I	- 6.952	36.82	52.6%	1.42
Study II	- 6.981	36.42	52.0%	1.43
Study III	- 1.131	24.61	35.1%	3.25
Experimental Result	~ - 24.30	~8.00	~11.5%	~1.25

From the comparative analysis, it is clearly evident that the modelled SAW filter response has a wider 3dB bandwidth and low insertion loss than the experimental result. Moreover, the spurious responses are rejected in the upper stopband. It has suppressed or removed by modifying the IDT structure in the SAW device. Thus, SAW filters became a small miniaturized size in practical applications. Therefore, it can be implemented in the mobile communication (GSM/CDMA/WCDMA) systems for perfect digital signal transceivers without any signal loss. Though these devices are implemented in amplifier circuit using electronic components, they are served as good low noise amplification as well as signals transceivers perfectly without noise and high power output. Thus, these SAW filter devices can also be used in wireless communication systems. The SAW filter device fabrication process is much complex than the other SAW devices. At present, the modelled results of the 70 MHz YZ-$LiNbO_3$ SAW filter device clearly shows that the device can acts as a *Low loss Wideband SAW filter* device. Therefore, only SAW filters can realize such unique functions in communication systems, and this technology will be hopefully applied to the practical application soon.

4. CONCLUSION

In the present work, a 70 MHz YZ-$LiNbO_3$ SAW filter had been successfully designed, modelled and simulated with the help of MATLAB®simulation tool by using different window functions, namely Hamming Window, Hanning Window and Sinc Window function. The insertion loss and 3dB bandwidth values of the modelled SAW filter devices had been compared

effectively with the experimental result available online. The modelled results show that the device responses with various window functions have a wide main lobe with minimum insertion loss. Therefore, the modelled device can be effectively used as a low loss wideband SAW filter device and hence these types of SAW filters are preferable for Digital Signal Processing (DSP) applications. Therefore, it is possible to obtain low loss wideband SAW filters with constant group delay, linear phase characteristic and good square shape of the absolute value of the transceivers ratio with the help of the obtained modelling results. These effects should be compensated for, especially in low loss filters, if the desired response is to be achieved.

REFERENCES

Atzeni, C., Masotti, L., Linear Signal Processing by Acoustic Surface-Wave Transversal Filters, *IEEE Trans. Microw. Theory Tech.*, 21(8), 505–519 (1973). https://dx.doi.org/10.1109/TMTT.1973.1128050

Bausk, E. V., Yakovkin, I. B., Design of low-shape-factor SAW filters having a single acoustic track, In: Proceedings of 1996 IEEE International Frequency Control Symposium. IEEE, 291–295 (1996).

Budreau, A. J., Temperature dependence of the attenuation of microwave frequency elastic surface waves in quartz, *Appl. Phys. Lett.* 18(6), 239 (1971). https://dx.doi.org/10.1063/1.1653647

Campbell, C. K., Applications of surface acoustic and shallow bulk acoustic wave devices, *Proc. IEEE* 77(10), 1453–1484 (1989a). https://dx.doi.org/10.1109/5.40664

Campbell, C. K., Applications of Surface Acoustic and Shallow Bulk Acoustic Wave Devices, *Proc. IEEE*77(10), 1453–1484 (1989b). https://dx.doi.org/10.1109/5.40664

Cooley, J. W., Tukey, J. W., An Algorithm for the Machine Calculation of Complex Fourier Series, *Math. Comput.* 19(90), 297 (1965). https://dx.doi.org/10.2307/2003354

Fall, D., Duquennoy, M., Ouaftouh, M., Piwakowski, B., Jenot, F., Modelling based on Spatial Impulse Response Model for Optimization of InterDigital Transducers (SAW Sensors) for Non Destructive Testing, *Phys. Procedia* 70, 927–931 (2015). https://dx.doi.org/10.1016/j.phpro.2015.08.192

Harris, F. J., On the use of windows for harmonic analysis with the discrete Fourier transform, *Proc. IEEE* 66(1), 51–83 (1978). https://dx.doi.org/10.1109/PROC.1978.10837

Hartmann, C. S., Bell, D. T., Rosenfeld, R. C., Impulse Model Design of Acoustic Surface-Wave Filters, *IEEE Trans. Microw. Theory Tech.* MTT-21(4), 162–175 (1973). https://dx.doi.org/10.1109/TMTT.1973.1127967

Hikita, M., Minami, K., Takimoto, H., Sakiyama, K., Investigation of attenuation increase at lower-side frequency bands for highly-integrated SAW modules, *Electron. Lett.* 42(25), 1488 (2006). https://dx.doi.org/10.1109/T-SU.1976.30868

Kaur, M., Sangeet, P. K., FIR Low Pass Filter Designing Using Different Window Functions and their Comparison using MATLAB, *Int. J. Adv. Res. Electr. Electron. Instrum. Eng.* 5(2), 753- (2016). https://dx.doi.org/10.15662/IJAREEIE.2016.0502016

Laker, K., Cohen, E., Szabo, T., Pustaver, J., Computer-aided design of withdrawal-weighted SAW bandpass filters, *IEEE Trans. Circuits Syst.* 25(5), 241–251 (1978). https://dx.doi.org/10.1109/TCS.1978.1084469

Luo, C., Gudem, P. S., Buckwalter, J. F., A 0.4–6-GHz 17-dBm B1dB 36-dBm IIP3 Channel-Selecting Low-Noise Amplifier for SAW-Less 3G/4G FDD Diversity Receivers, *IEEE Trans. Microw. Theory Tech.* 64(4), 1110–1121 (2016). https://dx.doi.org/10.1109/TMTT.2016.2529598

Morgan, D. R., Surface acoustic wave devices and applications: 1. Introductory review, *Ultrasonics*, 11(3), 121–131 (1973). https://dx.doi.org/10.1016/0041-624X(73)90608-2

Nyquist, H., Certain Topics in Telegraph Transmission Theory, *Trans. Am. Inst. Electr. Eng.* 47(2), 617–644 (1928). https://dx.doi.org/10.1109/T-AIEE.1928.5055024

Panasik, C. M., Hunsinger, B. J., Precise Impulse Response Measurement of SAW Filters, *IEEE Trans. Sonics Ultrason.* 23(4), 239–248 (1976). https://dx.doi.org/ 10.1109/T-SU.1976.30868

Parker, K., Apodization and windowing eigenfunctions, *IEEE Trans. Ultrason. Ferroelectr. Freq. Control* 61(9), 1575–1579 (2014). https://dx.doi.org/10.1109/TUFFC.2014.3071

Peach, R. C., Dix, C., A Low Loss Medium Bandwidth Filter on Lithium Niobate, In: 1978 Ultrasonics Symposium. IEEE, 509–512 (1978).

Peroulis, D., Loeches-Sánchez, R., Gómez-García, R., Psychogiou, D., Hybrid surface-acoustic-wave/microstrip signal-interference bandpass filters, *IET Microwaves, Antennas Propag.* 10(4), 426–434 (2016). https://dx.doi.org/10.1049/iet-map.2015.0346

Priya, R. B., Venkatesan, T., Pandya, H. M., A Comparison of Surface Acoustic Wave (SAW) Delay Line Modelling Techniques for Sensor Applications, *J. Environ. Nanotechnol.* 5(2), 42–47 (2016). https://dx.doi.org/10.13074/jent.2016.06.162193

Venkatesan, T., Haresh M, P., Surface Acoustic Wave Devices and Sensors - A Short Review On Design and Modelling by Impulse Response, *J. Environ. Nanotechnol.* 2(3), 81–89 (2013). https://dx.doi.org/10.13074/jent.2013.09.132034

Yatsuda, H., Yamanouchi, K., Automatic computer-aided design of SAW filters using slanted finger interdigital transducers, *IEEE Trans. Ultrason. Ferroelectr. Freq. Control* 47(1), 140–147 (2000). https://dx.doi.org/10.1109/5 8.818756